

## **Supplementary Information**

### ***In-Situ* Growth of CaMoO<sub>4</sub> on Electropolymerized PANI as Hybrid Electrocatalyst for Enhanced Oxygen Evolution**

*Nitika Garg,<sup>a</sup> Ashok K. Ganguli<sup>a,b\*</sup>*

<sup>a</sup>Department of Chemistry, Indian Institute of Technology Delhi, Hauz Khas, New Delhi  
110016, India

<sup>b</sup>Department of Chemical Sciences, Indian Institute of Science Education and Research  
Berhampur, Ganjam, Odisha-760003



Fig. S1: Digital picture of electrodeposited PANI electrode.

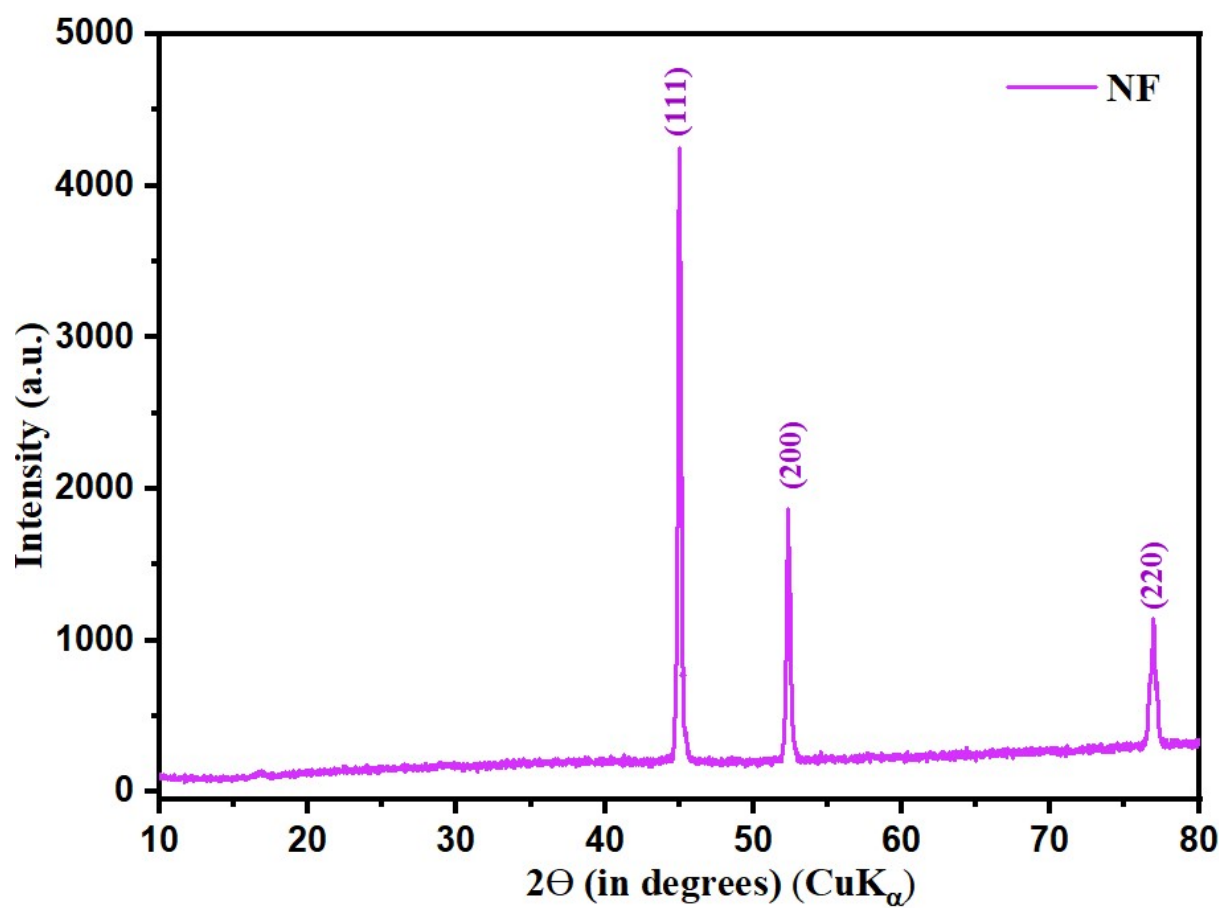
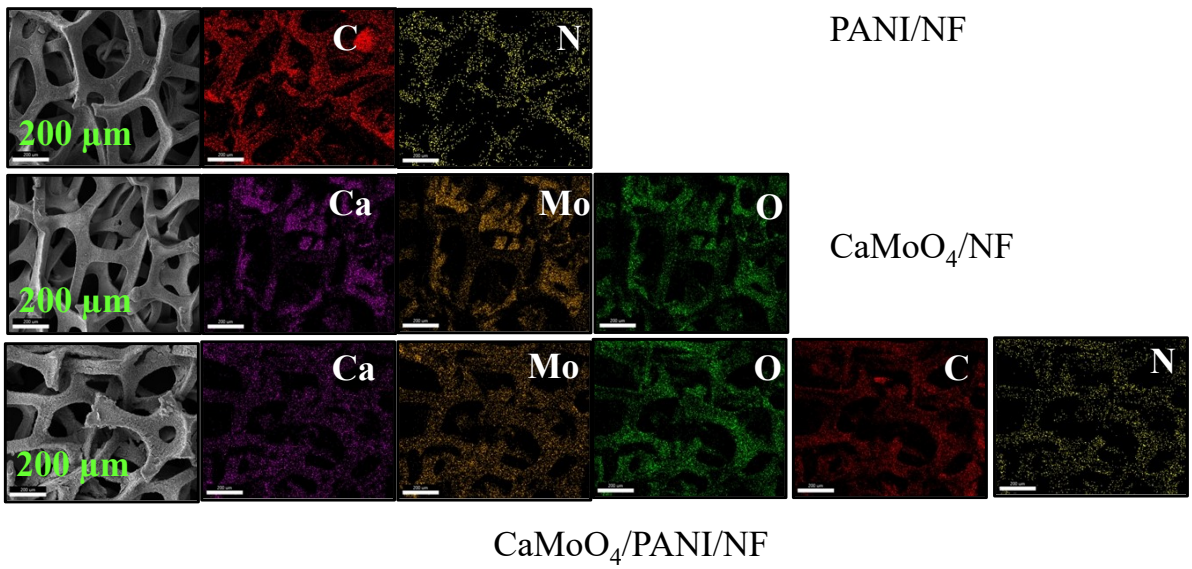
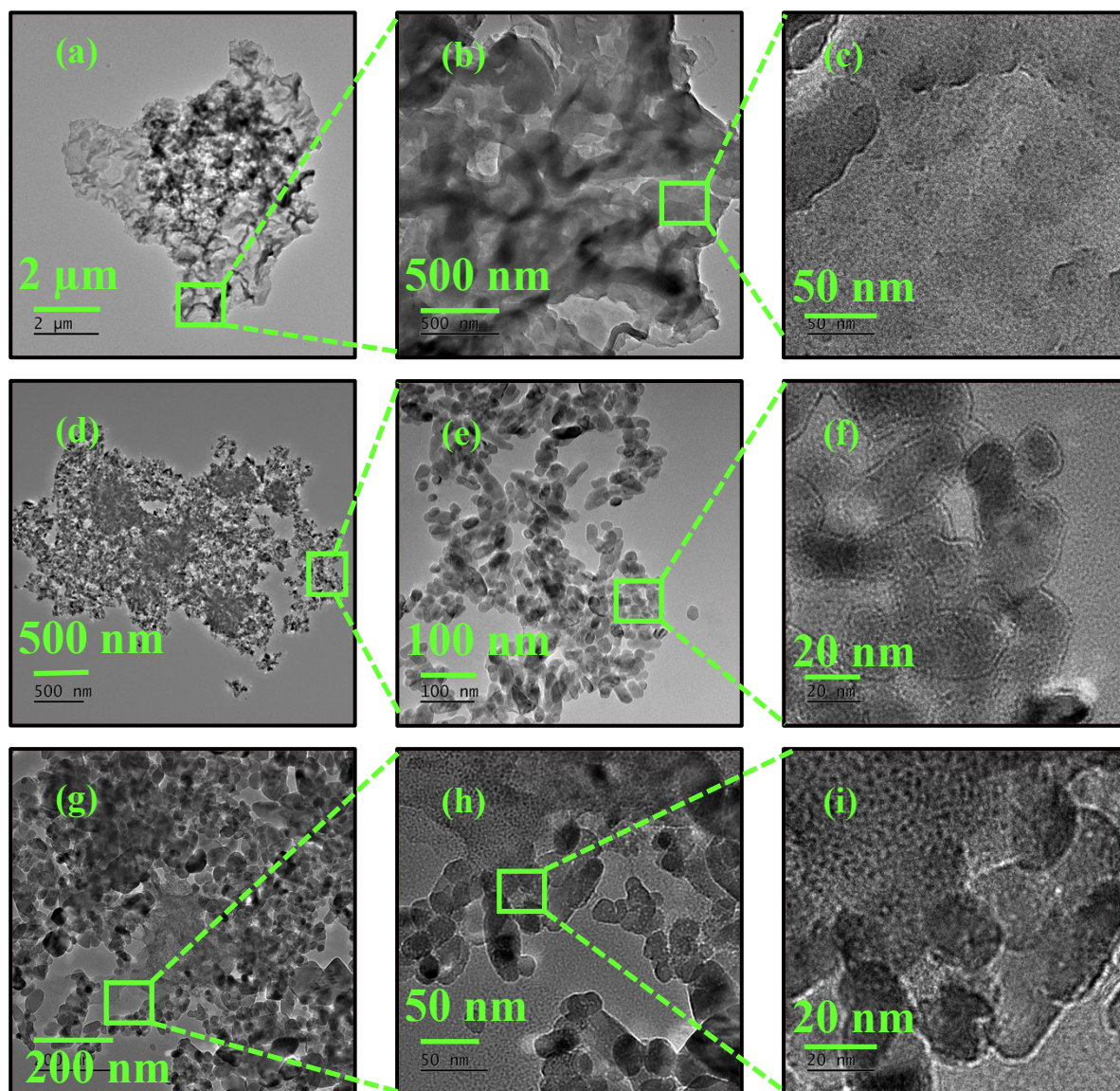


Fig. S2: PXRD pattern of bare nickel foam substrate.



**Fig. S3:** EDS analysis of (a) and (b) PANI, (c) and (d) CaMoO<sub>4</sub>, and (e) and (f) CaMoO<sub>4</sub>/PANI.



**Fig. S4:** TEM images of (a), (b) and (c) PANI, (d), (e) and (f) CaMoO<sub>4</sub>, and (g), (h) and (i) CaMoO<sub>4</sub>/PANI at different magnification.

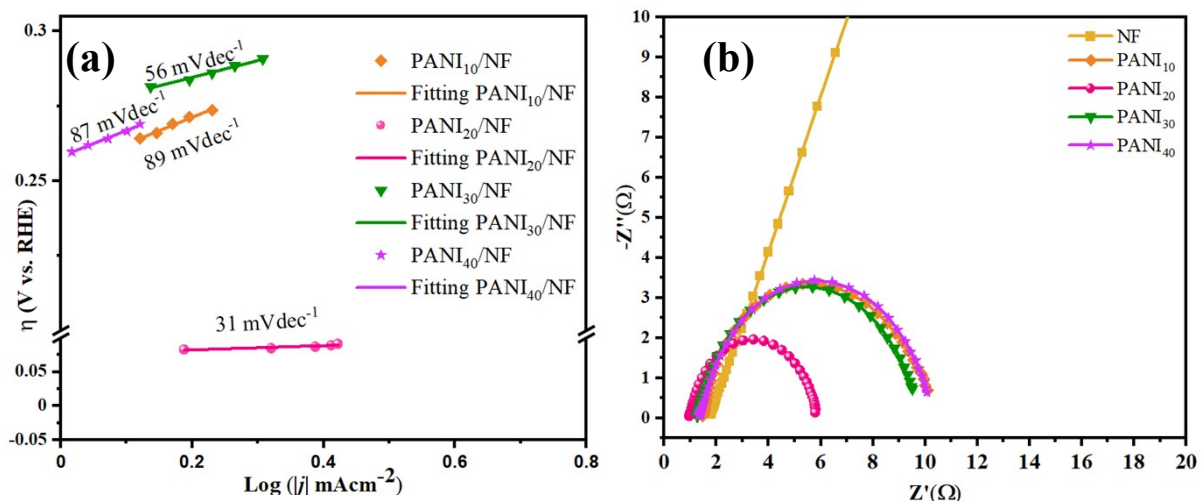


**Fig. S5:** (a) Tafel slope obtained from the polarization curves obtained using LSV measurements. (b) Nyquist plots.

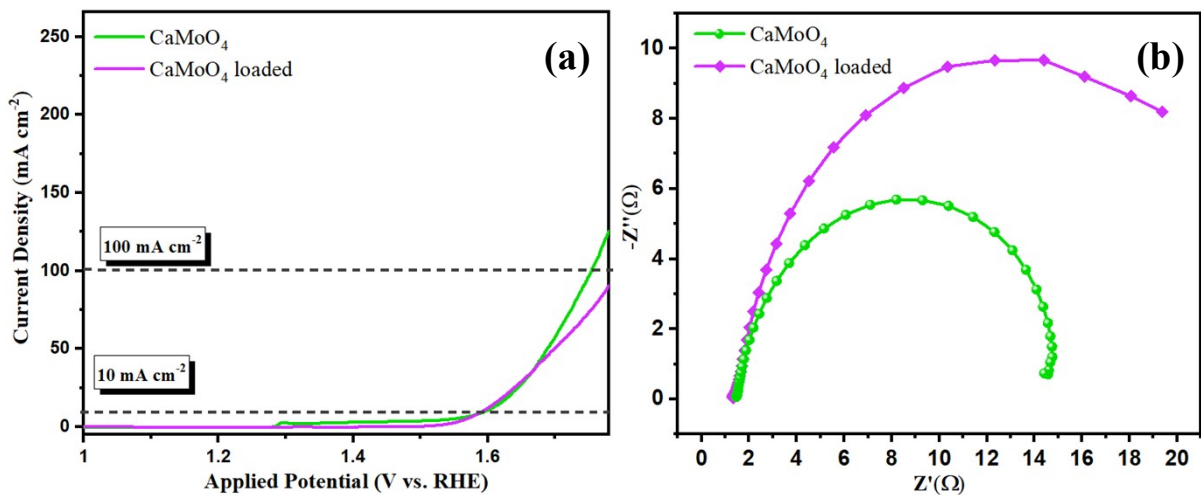


**Fig. S6:** (a) LSV curve and (b) Nyquist plot for comparison between binder-free CaMoO<sub>4</sub> electrode and CaMoO<sub>4</sub> electrode loaded on nickel foam using Nafion as binder.

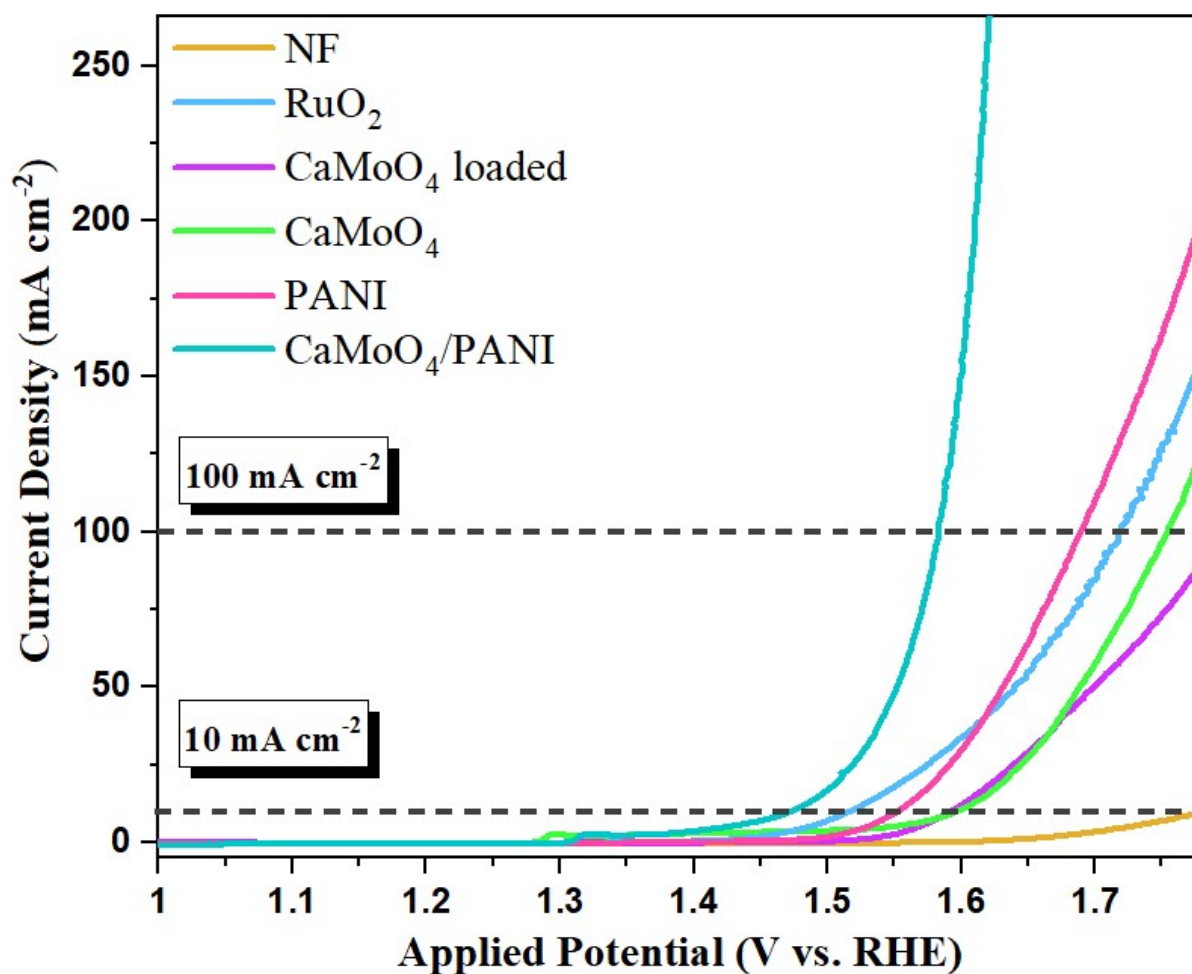


**Fig. S7:** LSV curves to compare OER activity of synthesized catalyst with noble metal catalyst ( $\text{RuO}_2$ ).

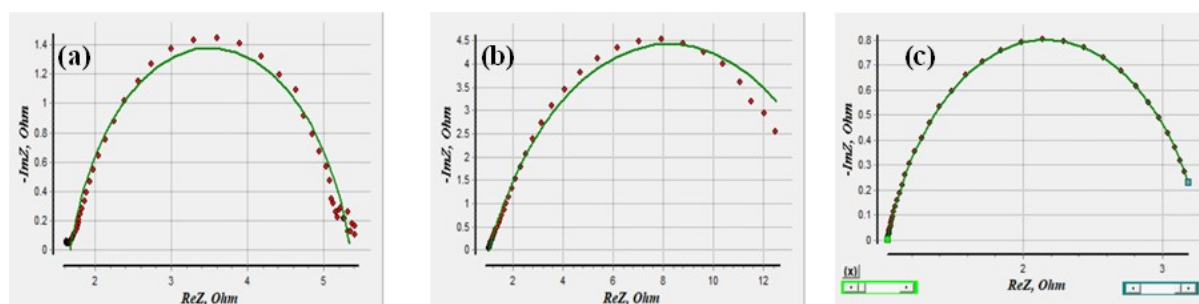


**Fig. S8:** Nyquist plots after circuit fitting (a) PANI, (b)  $\text{CaMoO}_4$  and (c)  $\text{CaMoO}_4/\text{PANI}$ .

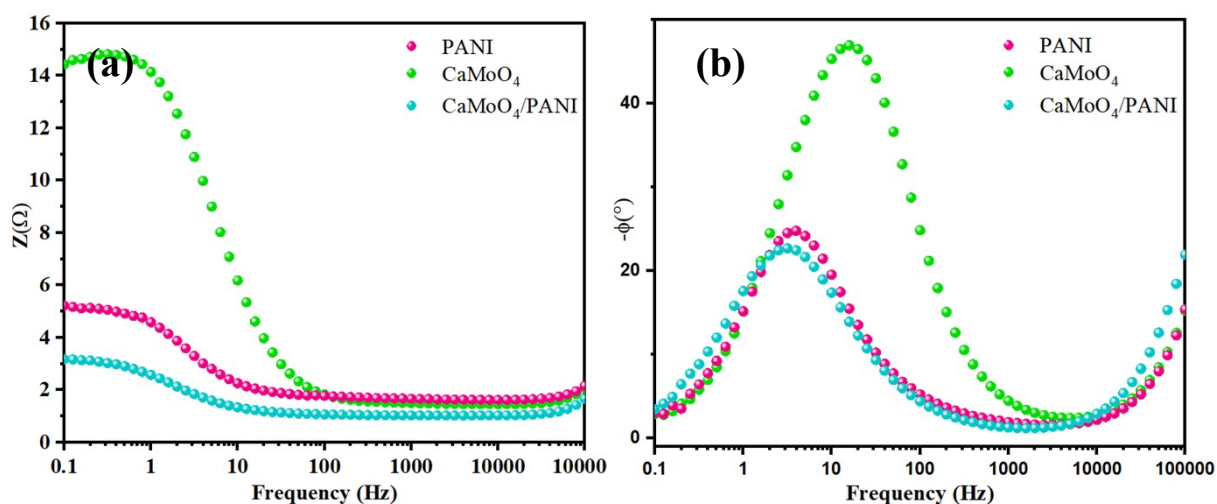


**Fig. S9:** (a) Bode plot ( $|Z|$  versus modulation frequency) and (b) Bode plot ( $\phi$  versus modulation frequency) of PANI, CaMoO<sub>4</sub>, and CaMoO<sub>4</sub>/PANI.

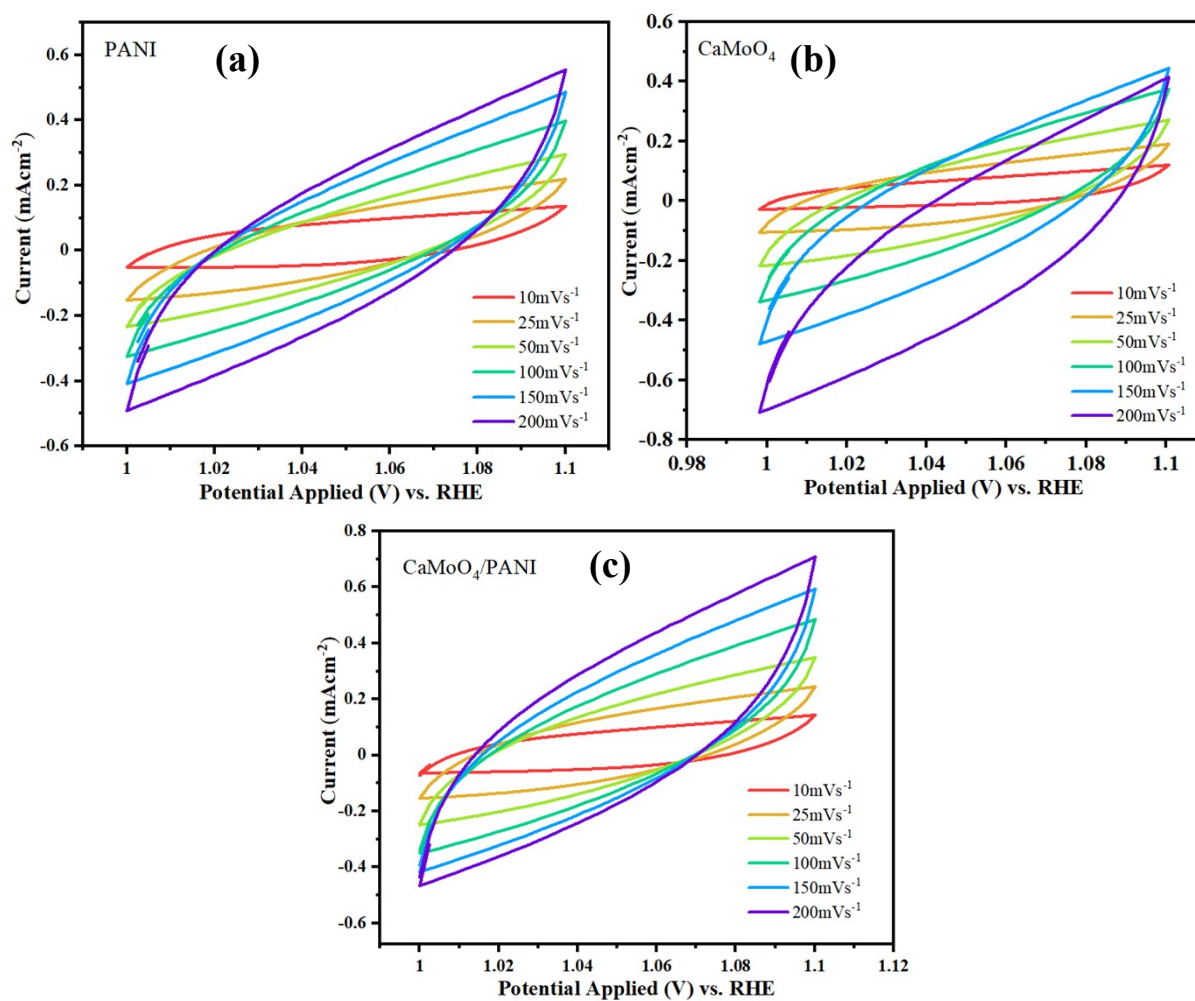


**Fig. S10:** CV curves for ECSA analysis in non-faradaic region of PANI, CaMoO<sub>4</sub>, and CaMoO<sub>4</sub>/PANI.

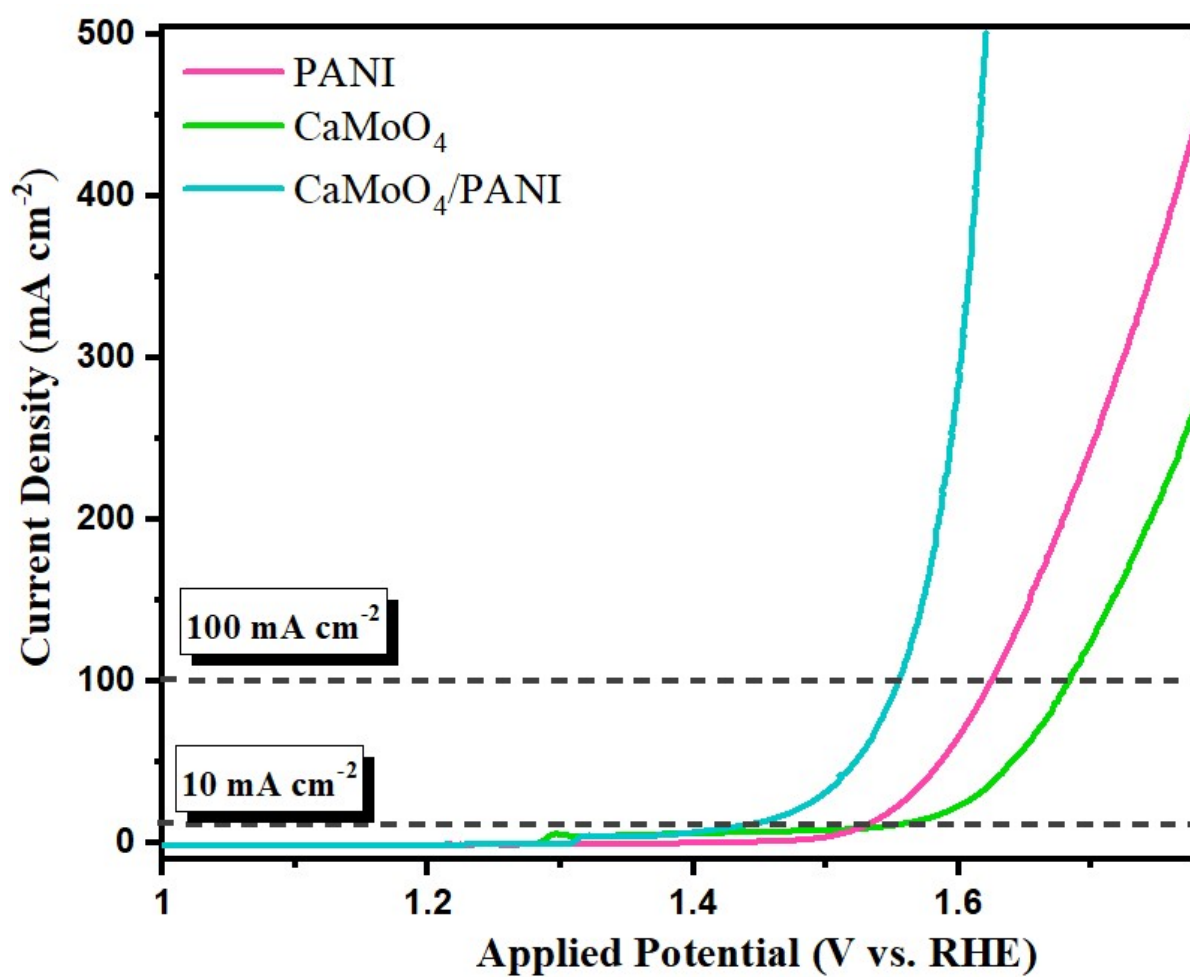
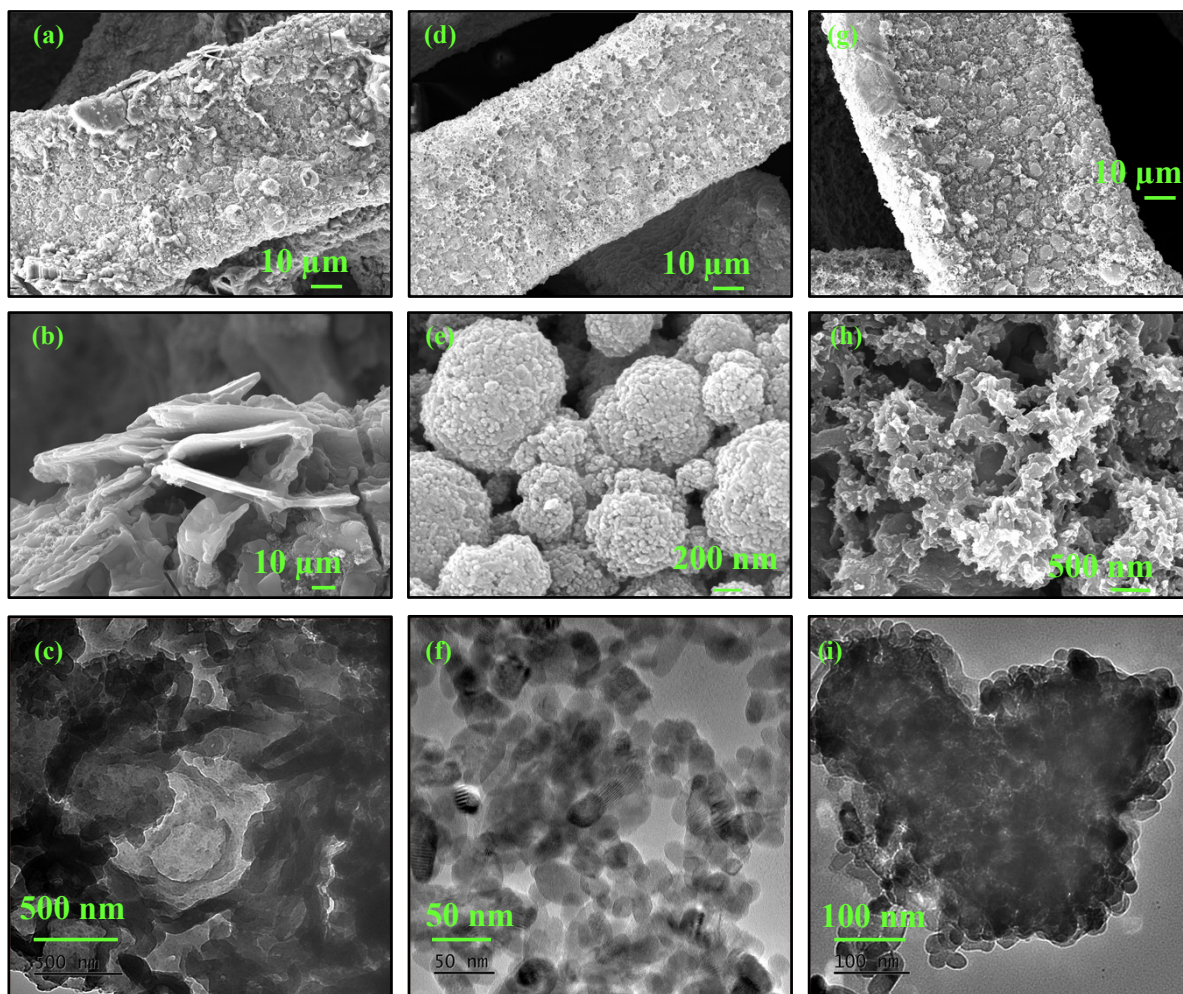
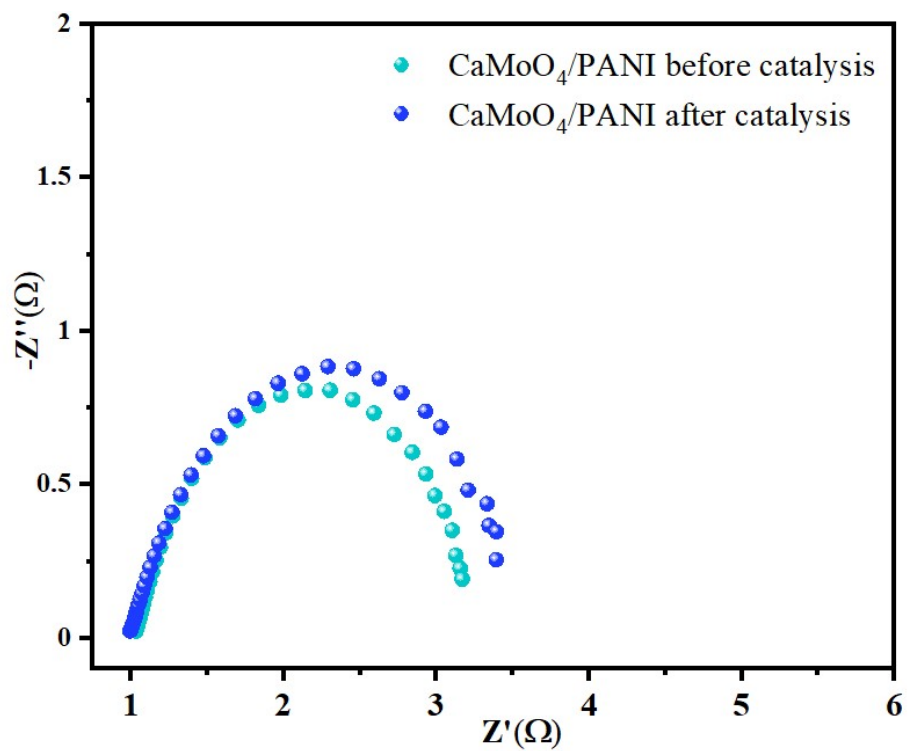


Fig. S11: ECSA corrected LSV curves of PANI, CaMoO<sub>4</sub> and CaMoO<sub>4</sub>/PANI.





**Fig. S12:** SEM and TEM images after catalysis (a), (b) and (c) PANI, (d), (e) and (f) CaMoO<sub>4</sub> and (g), (h) and (i) CaMoO<sub>4</sub>/PANI.



**Fig. S13:** Nyquist plot of  $\text{CaMoO}_4/\text{PANI}$  before and after catalysis

**Table 1:** OER electrocatalytic activity of PANI based previously reported catalysts in alkaline media

Catalyst	Substrate	$j$ (mAcm <sup>-2</sup> )	$\eta$ (mV)	References
CaMoO <sub>4</sub> /PANI	NF	10	233	This work
CaMoO <sub>4</sub>	NF	50	345	1
NiO/MnO <sub>2</sub> @PAN I	PG (pyrolytic graphite electrode)	10	345	2
PANI@Co-Fe LDHs	GC (glassy carbon electrode)	10	261	3
Co <sub>4</sub> Ni <sub>1</sub> @PANI	NF	10	288	4
CoFe <sub>2</sub> O <sub>4</sub> /PANI-MWCNTs	GC	10	314	5
NiFeLDH@PANi-CF	CF	100	380	6
PANI@NiO	NF	10	301	7
PANI coated Ni <sub>3</sub> Mo <sub>2</sub> P-MoO <sub>3</sub>	NF	100	290	8
CoMoS-PANI	NF	10	250	9

**References:**

- 1 Y. Gou, Q. Liu, X. Shi, A. M. Asiri, J. Hu and X. Sun, *Chem Commun.*, 2018, **54**, 5066–5069.
- 2 J. He, M. Wang, W. Wang, R. Miao, W. Zhong, S.-Y. Chen, S. Poges, T. Jafari, W. Song, J. Liu and S. L. Suib, *ACS Appl. Mater. Interfaces*, 2017, **9**, 42676–42687.
- 3 X. Sun, X. Liu, R. Liu, X. Sun, A. Li and W. Li, *Catal. Commun.*, 2020, **133**, 105826.
- 4 V. Ashok, S. Mathi, M. Sangamithirai and J. Jayabharathi, *Energy & Fuels*, 2022, **36**, 14349–14360.
- 5 Y. Liu, J. Li, F. Li, W. Li, H. Yang, X. Zhang, Y. Liu and J. Ma, *J. Mater. Chem. A*, 2016, **4**, 4472–4478.
- 6 N. Lingappan, I. Jeon and W. Lee, *J. Mater. Chem. A*, 2023, **11**, 17797–17809.
- 7 J. Zhang, Y. Cao, H. Xu, X. Liu, J. Gong, Y. Tong, G. Zhang, Y. Li, C. Tong and Z. Li, *J. Phys. Chem. Lett.*, 2024, 4088–4095.
- 8 J. Teng, D. Liu, X. Zhang and J. Guo, *J. Electroanal. Chem.*, 2022, **908**, 116129.
- 9 S. Mathew, J.-H. Sim, R. Rajmohan, O. L. Li and Y.-R. Cho, *Electrochim. Acta*, 2022, **403**, 139586.